2020

PERFLUOROOCTANESULFONIC ACID (PFOS) AS A POTENTIAL RISK FACTOR FOR LATE-ONSET ALZHEIMER'S DISEASE

Veronia Basaly
University of Rhode Island, veroniabasaly@gmail.com

PERFLUOROOCTANESULFONIC ACID (PFOS) AS A POTENTIAL RISK FACTOR FOR LATE-ONSET ALZHEIMER'S DISEASE

BY

VERONIA BASALY

A THESIS SUBMITTED IN PARTIAL FULFILLMENT OF THE

REQUIREMENTS FOR THE DEGREE OF

MASTER OF SCIENCE

IN

PHARMACEUTICAL SCIENCES

UNIVERSITY OF RHODE ISLAND

2020

MASTER OF SCIENCE THESIS

OF

VERONIA BASALY

APPROVED:

Thesis Committee:

Major Professor Nasser Zawia

Angela Slitt

Lisa Weyandt

Brenton DeBoef
DEAN OF THE GRADUATE SCHOOL

UNIVERSITY OF RHODE ISLAND
2020

ABSTRACT

Alzheimer's disease (AD) is a progressive neurodegenerative disorder that accounts for about 60 to 80% of dementia cases worldwide. AD is characterized by two important physiological features: extracellular senile plaques consisting of β-amyloid (Aβ) peptide that is cleaved from a larger protein called the amyloid precursor protein (APP), and intracellular neurofibrillary tangles (NFTs) containing hyperphosphorylated tau protein. The pathogenesis of sporadic or late-onset AD (LOAD) which represents 95% of the cases appears to not be heritable and may be related to epigenetic programming and environmental factors acquired earlier in life. Apolipoprotein allele 4 (ApoE4) protein is encoded by the ApoE gene and is considered the only established genetic risk factor for LOAD. It is suggested that ApoE4 affects the pathogenesis of AD by increasing tau hyperphosphorylation, inhibiting the clearance of amyloid-β (Aβ), and promoting Aβ aggregation. Perfluorooctanesulfonic acid (PFOS) is a persistent organic pollutant known to cause neurotoxicity and poses a major threat to the ecosystem and human health. The aim of this study was to investigate PFOS as a potential risk factor for LOAD by assessing the potential mechanism and impact of PFOS on three major AD-associated pathways: amyloidogenesis, tau pathology, and ApoE using *in vivo* and *in vitro* models. Our findings demonstrated that SH-SY5Y neuroblastoma cells exposed to low concentrations of PFOS showed increased protein levels of APP, tau, and phosphorylated tau (p-tau) at Ser-404 and Thr-181 sites. PFOS exposure also caused an elevation in the kinase GSK3β, ApoE4 protein levels in vitro; however, only GSK3β and ApoE were modulated *in vivo*. These data suggest that ApoE4 is inducible by

environmental exposure to PFOS and may play a role in AD pathogenesis primarily by modulating the tau pathway via a mechanism that involves GSK3β.

Keywords: PFOS, ApoE4, Late-onset Alzheimer's disease, amyloidogenic pathway, Tau pathology, glycogen synthase kinase-3 beta (GSK3β).

ACKNOWLEDGMENTS

I would like to thank my major professor Dr. Nasser Zawia for giving me the opportunity to join his lab and for his guidance and support through this journey. I would like to express my sincere appreciation to my committee members, Dr. Angela Slitt and Dr. Lisa Weyandt for their support, suggestions, and encouragement, and Dr. Rainer Lohmann for chairing my defense. I also want to thank my lab members, Dr. Syed Bihaqi, Jaunetta Hill, and Abdullah G. Alharbi for their advice, support, and for always being there when needed. A special thanks to Dr. Haripriya Vittal Rao for her continuous support, valuable advice, guidance, and for always being there for me.

I would like to thank the Sources, Transport, Exposure, and Effects of PFAS (STEEP), an NIH funded superfund group for funding this project. Also, I would like to extend my gratitude to the Fulbright Student Scholarship program for their continuous support and for generously funding me during my stay in the United States.

Finally, I am grateful for my friends who have provided their support and helped me get through the toughest challenges of being an international graduate student. I am thankful for my family and my parents especially my sisters for their continuous support. To the most important person in my life, my mother, my role model, whom without her I would not be here, thank you for all your support, encouragement, patience, and for raising me to become the person who I am today. I have been blessed with this amazing support system which helped me to reach this point.

PREFACE

This thesis was written in a manuscript format according to the University of Rhode Island Graduate School guidelines and consists of one manuscript that satisfy the requirements of the Department of Biomedical and Pharmaceutical Sciences, College of Pharmacy, University of Rhode Island.

MANUSCRIPT: Perfluorooctanesulfonic acid (PFOS) as a potential risk factor for late-onset Alzheimer's disease. This manuscript has been prepared for submission to "Toxicology and Applied Pharmacology".

TABLE OF CONTENTS

LIST OF FIGURES

MANUSCRIPT – I

Prepared for submission to Toxicology and Applied Pharmacology

Perfluorooctanesulfonic acid (PFOS) as a potential risk factor for late-onset Alzheimer's disease

Veronia Basaly[1], Jaunetta Hill[1], Syed Bihaqi[1], Emily Marques[1], Angela L. Slitt[1] and Nasser Zawia[1,2,3]

[1]Department of Biomedical and Pharmaceutical Sciences, College of Pharmacy, University of Rhode Island, Kingston, RI, 02881, USA

[2]Geroge and Anne Ryan Institute for Neuroscience, University of Rhode Island, Kingston, RI, 02881, USA

[3]Interdisciplinary Neuroscience Program, University of Rhode Island, Kingston, RI, 02881, USA

Corresponding Author:

Nasser Zawia, Ph.D.

Department of Biomedical and Pharmaceutical Sciences

University of Rhode Island

7 Greenhouse Road, Kingston, RI 02881

Phone: 401-874-5368

E-mail: nzawia@uri.edu

INTRODUCTION

Alzheimer's disease (AD) is a progressive neurodegenerative disorder that accounts for about 60 to 80% of dementia cases worldwide[1,2]. Several pathologies have been implicated with AD including neuroinflammation, microglia activation, and oxidative stress[3]. The major AD hallmarks are the presence of extracellular senile plaque consisting of β-amyloid (Aβ) peptide that is cleaved from a larger protein called the amyloid precursor protein (APP), and intracellular neurofibrillary tangles (NFTs) containing hyperphosphorylated tau protein[4]. Tau is the major neuronal intracellular microtubule binding protein, it is essential for stabilization of microtubules, and axonal transport in neurons[5]. Hyperphosphorylated tau which occurs in pathological conditions, reduces tau affinity to microtubules and impairs axonal transport[6,7]. Several protein kinases are involved in the phosphorylation of tau protein such as the proline-directed protein kinases: cyclin-dependent kinase-5 (CDK5) and glycogen synthase kinase-3 beta (GSK3β)[8].

The etiology of Late-onset Alzheimer's Disease (LOAD) which represents 95% of the cases is sporadic in nature and the only established gene associated with LOAD is Apolipoprotein (ApoE)[9]. Mounting evidence has indicated that the human ApoE gene is the strongest genetic risk factor for the development of LOAD[10,11]. The presence of one copy of ApoE4 allele increases the risk of acquiring LOAD by about 3 times while the risk is increased by 15-fold if 2 copies of ApoE4 allele are present[9,11]. In the central nervous system (CNS), ApoE is involved with the repair process after injury[10], it functions as a lipid transporter and/ or signaling molecule[12,13]. There are 3 different isoforms of ApoE in humans, however, ApoE4 is the one mainly associated with increased prevalence of AD[9,10,14]. Previous studies have reported that fragments of ApoE4 accumulated in NFTs in

brains of AD patients[15], and are detected in neurons of ApoE4 transgenic mice[16]. ApoE4 appears to result in behavioral deficits and neurodegeneration through disruption of the cytoskeleton, stimulation of tau phosphorylation, generation of NFTs[17,16,18] as well as by interfering in Aβ clearance thereby facilitating the aggregation of Aβ and formation of senile plaque[9,10,11,17,19,20,21].

The random nature of LOAD suggests that environmental factors may contribute to the onset of LOAD, particularly environmental exposures acquired earlier in life[22]. Poly- and perfluoroalkyl substances (PFASs) are a class of emerging persistent organic pollutants (POPs) with neurotoxic properties. They are manmade fluorinated chemicals that have been widely used in numerous industrial and consumer products such as textile products, firefighting foams, and oil-resistant coatings for paper products. PFASs persist in the environment and bioaccumulate in the food chain [23]. One of the most widely used PFASs is the 8-carbon chain (C8) Perfluorooctanesulfonic acid (PFOS) which has been detected in adult human serum[24] and in children with a serum concentration equal or even higher than adults[25]. PFOS can cross the placenta, the blood brain barrier (BBB)[26,27,28]and was found in breast milk [29]. PFOS strongly binds to plasma albumin[30] and it has an average serum half-life of 5.4 years in humans [31], and 36.9 days for CD-1 mice[32].

Even though levels of PFOS exposure have decreased during the last decade due to industrial pashing out of PFOS, it persists in the environment due to its resistance to photolysis, hydrolysis, and biodegradation[23]. Developmental studies using rodents showed that exposure to PFOS can cause neural damage manifested by chronic glial activation, release of inflammatory factors[33], altered susceptibility of the cholinergic system, resulting in behavioral deficits, reduced spatial learning, memory and cognitive impairment which

can persist into adulthood [34,35,36,37]. Neonatal exposure of mice to a single PFOS dose 21μmol/kg body weight (11.3 mg/kg body weight) on PND 10 increased cerebral tau protein expression and caused behavioral abnormalities in adult mice [34, 37,38]. Moreover, PFOS resulted in an increase in β-amyloid aggregation, increased tau levels, and tau hyperphosphorylation in adult rats[39] suggesting an association between developmental PFOS exposure and LOAD.

Therefore, the main aim of this study was to investigate the potential of PFOS exposure as a risk factor for LOAD by assessing its impact on biomarkers associated with three major AD-related pathways in an *in vitro* model using the human SH-SY5Y neuroblastoma cell line. Furthermore, the same pathways were examined following developmental PFOS exposure in timed-pregnant CD-1mice.

MATERIALS AND METHODS

Animal model and PFOS exposure

Twelve timed-pregnant CD-1 mice were purchased from Charles River Laboratories (Wilmington, MA). The pregnant dams were received on gestation day 1 (GD)1 at the University of Rhode Island (URI) Comparative Biology Resource Center (CBRC). Upon arrival, the dams were weighed and housed individually in a designated room with controlled temperature (20-26°C), relative humidity (30-70%), and 12:12 hour light-dark cycle (light on at 6:00 AM; light off at 6:00 pm) where standard chow diet (SD; Teklad Extruded global diet, 2020X) and water were provided *ad-libitum*. Dams were randomly assigned into two treatment groups (n= 6 per treatment group) and were dosed with either vehicle (0.5% Tween-20 in deionized water) or 1 mg/kg/day PFOS (396575, Sigma Aldrich, St. Louis, MO) dissolved in deionized water with 0.5% Tween-20 via oral gavage throughout gestation (GD1-GD18 or 19 [birth]) and lactation (birth to postnatal day [PND] 20) as shown in figure 1.

For dose calculation, the dams body weights were recorded every 3-4 days and the last dose given was on PND 19. On PND 1, neonates were randomly assigned to dams within the same treatment group with 10 pups assigned to each dam in order to ensure equal lactational PFOS exposure, excess pups were culled. On PND 20, dams and pups were fasted for 4-6 hours and euthanized via cardiac puncture with subsequent decapitation. The brain tissues were collected and stored at -80°C for biomarker assessment. During this study, the animals were under the supervision of the URI CBRC staff. The animal protocols and the study procedures were reviewed and approved by the University of Rhode Island Institutional (URI) Animal Care and Use Committee (IACUC).

Cell culture

Human neuroblastoma SH-SY5Y cells were purchased from American Type Culture Collection (ATCC, Manassas, VA). Cells were cultured in Dulbecco's Modified Eagle Medium (DMEM)/F12 (Invitrogen, MD) supplemented with 10% fetal bovine serum (FBS) (Thermo Scientific, Waltham, MA), 100 U/ml penicillin, 100 µg/ml streptomycin, and 2 mM L-glutamine (Sigma Aldrich, St. Louis, MO) in T-75 tissue culture flasks with vented lids (Cyto-one, USA Scientific) in a CO_2 incubator maintained at 5% CO_2 and 37°C. Cells were then sub-cultured at a density of 10^5 cells/mL into a six-well plate and upon 80% confluency, cells were differentiated for 6 days using 10 µM all-trans retinoic acid (Sigma Aldrich, St. Louis, MO) dissolved in DMEM/F12 medium containing 1% FBS, 100 U/ml penicillin, 100 µg/ml streptomycin in the dark. Cells were observed for neurite out-growth with media being changed every 48 hours as described previously[40]. Furthermore, differentiated cells were exposed to PFOS dissolved in DMSO for 24, 48, and 72 hours at 37°C with the following concentrations: 0, 0.001, 0.1, 5, 25, 50, 100 µM. The concentration of DMSO in the cell culture media was maintained at 0.1% for control and across all treatment groups.

MTS assay

The viability of differentiated SH-SY5Y human neuroblastoma cells was assessed after exposure to PFOS using the MTS assay kit (Promega, Madison, WI). The cells were seeded in 96-well plate (2 x 10^4 cells/well) and treated with different concentrations of PFOS ranging from 0-100 µM for 24, 48, and 72 hours. After the completion of the incubation period, the media containing PFOS was aspirated out and fresh media with no PFOS was added in each well followed by treatment with 20 µl of MTS solution. The plates

were incubated at 37°C for 2 hours and after incubation, the absorbance was measured at 490nm by using the Spectramax M2 Multi-mode microplate reader (Molecular Devices, San Jose, CA).

Protein Extraction and Western Blotting

The brain cortex samples and cells were lysed using radio-immunoprecipitation assay (RIPA) lysis buffer (Sigma Aldrich, MO) supplemented with phosphatase and protease inhibitor tablet: one tablet was dissolved in 10 ml of RIPA buffer (Pierce Protease and Phosphatase Inhibitor Mini Tablets, EDTA-Free, Thermo Scientific, Waltham, MA). The samples were incubated on ice for 30 min, then vortexed and sonicated for 5 minutes. The samples were subsequently centrifuged at 10,000 g for 20 min and the supernatants were collected and stored at -80°C for protein quantification and western blot analysis. The protein concentration was determined using Micro BCA protein assay kit (Thermo Scientific, Waltham, MA). For western, at least 20 µg of total protein was first separated by sodium dodecyl sulfate polyacrylamide gels (SDS-Page) on 4-15% Mini-protean® TGX™ precast gels (Bio-Rad, Hercules, CA), and then transferred to polyvinylidene fluoride (PVDF) membranes (GE-Healthcare, Piscataway, NJ). The membranes were blocked for 1 hour at room temperature with gentle agitation in blocking buffer comprising 5% (w/v) bovine serum albumin (BSA) in Tris-Buffered saline with 0.1% Tween-20 (TBST, pH 7.4).

Immunoblotting was then performed by incubating the membranes with gentle agitation on a shaker overnight at 4°C with primary antibodies of interest: Rabbit Anti-ApoE (Thermo Scientific, Waltham, MA), Mouse Anti-ApoE4, Mouse Anti-Tau-46, Rabbit Anti-Ser404, Rabbit Anti-Thr181, Rabbit Anti-GSK3β, Rabbit Anti-CDK5, Rabbit

Anti-APP (Cell Signaling Technology, MA) at a dilution of 1:1000 in TBST. On the following day, the membranes were washed three times with TBST for 5 min each and exposed at room temperature for 1 hour to either goat anti-mouse or goat anti-rabbit IRDye® 680 or 800 LT infrared dye (LI-COR Biotechnology, Lincoln, NE) at a 1: 10,000 dilution factor in TBST then the membranes were again washed three times with TBST. Also, the specific target protein/GAPDH ratio was obtained by re-probing the membranes for 2 hours at room temperature with primary antibody for the protein Glyceraldehyde 3-phosphate dehydrogenase (Rabbit Anti-GAPDH) at 1:5,000 dilution as a control, followed by washing and re-exposure to goat anti-rabbit IRDye® 680 or 800 LT infrared dye (LI-COR Biotechnology, Lincoln, NE) at a 1: 10,000 dilution factor in TBST (Cell Signaling Technology, MA). Finally, images were captured using the Odyssey® Infrared Imaging System (Li-Cor, NE), and Band intensities were measured using NIH ImageJ software and normalized against GAPDH.

Total RNA isolation, synthesis of cDNA, and RT-q PCR

Total RNA was isolated from cerebral cortex tissues and the SH-SY5Y cells using the TRIzol reagent method (Invitrogen, Carlsbad, CA). The integrity of the isolated RNA was verified by NanoDrop (Thermo Scientific, Wilmington, DE) analysis. The complementary DNA (cDNA) was then synthesized following the manufacturer's instruction by using the iScript™ Select cDNA synthesis kit (Bio-Rad, Hercules, CA). The reaction mixture consisted of 1µg of RNA diluted in 4 µl 5X iScript reaction mix, 1 µl iScript reverse transcriptase in a total volume of 20 µl of RNA free water. Using MJ Research MiniCycle™ (Bio-Rad, Hercules, CA) the samples were incubated for 26

minutes using the following protocol, Priming for 5 min at 25^{o}C, reverse transcription at 46 ^{o}C for 20 min, RT inactivation 1 min at 95 ^{o}C.

Primer pairs for mouse tau, APP, GSK3β, CDK5, GAPDH and human tau, APP, GSK3β, CDK5 and GAPDH were obtained from integrated DNA Technologies IDT (Coralville, IA, USA) as follows: mouse tau F: 5'-CCTGAGCAAAGTGACCTCCAAG-3'; and tau R: 5'-CAAGGAGCCAATCTTCGACTGG-3'; mouse APP F: 5'-TGCAGC AGAACGGATATGAG-3'; and APP R: 5'-ACACCGATGGGTAGTGAAGC-3'; mouse GSK3β F: 5'-AGGAAGGAAAAGGTGATTCAAGA-3'; and GSK3β R: 5'-TGCTGCCA TCTTTATCTCTGCT-3'; mouse CDK5 F: 5'-GGGACCTGTTGCAGAACCTAT-3'; and CDK5 R: 5'-AGTCAGAGAAGTAGGGGTGCT-3'; mouse GAPDH F: 5'-TGGTGA AGCAGGCATCTGAG-3'; and GAPDH R: 5'-TGCTGTTGAAGTCGCAGGAG-3′; human tau F: 5'-TGAACCAGGATGGCTGAGC-3', and tau R: 5'-TTGTCATCGCTTC CAGTCC-3'; human APP F: 5'-CTGTGGCAGACTGAACATGC-3', and APP R: 5'-TGTTCAGAGCACACCTCTCG-3'; human GSK3β F: 5'- GGATTCGTCAGGAACAG GACA-3', and GSK3β R: 5'-AGTATTAGCATCTGACGCTGC-3'; human CDK5 F: 5'-GATGATGAGGGTGTGCCGAG-3', and CDK5 R: 5'-TGCGGCTATGACAGAATCC C-3'; human GAPDH F: 5'-AGGTCGGAGTCAACGGATTT-3', and GAPDH R: 5'-TTCCCGTTCTCAGCCTTGAC-3'. Real-time PCR was carried out in 20 µl reaction volumes containing 1 µl of each forward and reverse primers, 1 µl of cDNA, 7 µl of nuclease-free water, and 10 µl of SYBR® Green PCR Master Mix (Applied Biosystems, Foster City, CA). The qPCR reaction was performed following the standard protocol: samples were incubated for 2 min at 50°C, then for 10 min at 95°C, followed by 15 seconds at 95°C for 40 cycles and for 1 min at 60°C By using the ViiA7 real-time PCR system

(Applied Biosystems, Foster City, CA). GAPDH mRNA expression was used as the endogenous control and the data was reported using the $2^{-\Delta\Delta CT}$ method.

Enzyme Linked Immunosorbent Assay (ELISA)

Cortex tissues were weighed and homogenized in eight volumes of an ice-cold solution containing 5 M guanidine HCl dissolved in 50 mM Tris-HCl, PH 8.0 (Sigma Aldrich, St. Louis, MO). The mixture was maintained for 3-4 hours at room temperature and then diluted with ice-cold Phosphate buffer saline (PBS) supplemented with 1X protease and phosphatase inhibitor (Thermo Scientific, Waltham, MA) until reaching a final concentration of 0.1 M guanidine. The samples were centrifuged for 20 minutes at 16,000 g at 4°C and the resulting supernatant was maintained either on ice for Aβ quantification or stored at -80°C for later use. ELISA kit catalog numbers KMB3441 and KMB3481 (Thermo Scientific, Waltham, MA) were used according to the manufacturer's instruction for quantification of $A\beta_{1-42}$ and $A\beta_{1-40}$ respectively.

These ELISA kits contain a colorimetric detection with double ELISA antibody approach. In each kit, the N-terminus of the mouse Aβ is determined by the monoclonal antibody coated in the wells. The Standards (provided in the kit) and the samples containing the Aβ antigen were added to the wells with the appropriate dilution (100 µl in each well). The plates were maintained at room temperature for 2 hours to allow the binding of the immobilized (capture) antibody and the Aβ antigen. Then, the plates were washed four times by using the washing solution provided in the kit. Subsequently, a solution of rabbit antibody specific for the C-terminus of either $A\beta_{1-42}$ or $A\beta_{1-40}$ was added to the wells (100 µl in each well) except for the blanks. The plates were then covered and incubated again for 1 hour at room temperature. After incubation, the wells were washed 4X using the

washing solution and 100 µl of horseradish-peroxidase-labeled anti-rabbit antibody was added to each well except for the blanks. Then, the plate was covered and incubated at room temperature for 30 minutes followed by four times washing. Then, 100 µl of the stabilized chromogen solution was added to each well and the plate was incubated at room temperature for 20-30 minutes in the dark. Once, the reaction mixtures turned blue, 100 µl per well of the stop solution was added to each well to stop the reaction and the mixture turned yellow. Finally, the absorbance was detected at 450 nm using the Spectramax M2 Multi-mode microplate reader (Molecular Devices, San Jose, CA)

Statistical analysis

The results of various exposed groups versus the control were expressed as the mean ± the standard error of the mean (SEM). The data were analyzed by using the statistical tests: unpaired two-tailed Student's t-test for comparison between two groups and the one-way analysis of variance (ANOVA) followed by the Dunnett or Tukey test for multigroup comparisons. The GraphPad Prism 8.0 computer software (La Jolla, CA, USA) was used for the analysis, and p-value < 0.05 was considered to indicate a statistically significant difference.

RESULTS

Effects of PFOS exposure on SH-SY5Y cell viability

Differentiated SH-SY5Y cells were exposed to a series of PFOS concentrations (0, 0.001, 0.1, 1, 5, 25, 50, 100 µM) and cell viability was determined using the MTS assay following 24, 48, and 72 h of exposure. At 24h, There was no significant cytotoxicity observed. However, at 48 (100 µM) and at 72 h (25, 50, 100 µM) concentrations of PFOS revealed significant decreases in cell viability (p= 0.05, p< 0.001). Thus, PFOS exposure at concentrations (0.001, 0.1 µM) for 24 h were considered appropriate for further studies (Figure 2).

PFOS effects on APP mRNA and protein levels in differentiated SH-SY5Y cells. (amyloidogenic pathway)

Further, we investigated the effects of PFOS on AD biomarkers related to the amyloidogenic pathway in human neuroblastoma SH-SY5Y cells. APP protein level was significantly elevated as compared to the control after 24 h exposure to 0.001 µM concentration of PFOS, p= 0.0152 (Figure 3A, B). We did not observe any effects on APP mRNA levels (Figure 3C).

PFOS effects on Tau mRNA expression, Total Tau, and P-tau protein levels in differentiated SH-SY5Y cells (tau Pathway)

SH-SY5Y cells showed a significant increase in total tau, P-tau (Ser-404) and P-tau (Thr-181) protein levels as compared to controls after 24 h exposure to 0.001 µM of PFOS, P= 0.0307, P= 0.0062, P=0.036 respectively (Figure 4A, B, D-G). Also, P-tau (Ser-404) was significantly elevated as compared to controls in SH-SY5Y cells after 24 h exposure to 0.1 µM of PFOS, P= 0.0058 (Figure 4D, E). Based on one-way ANOVA, there

was no effect of PFOS exposure on total tau mRNA expression (Figure 4C). Next, we investigated the effect of PFOS on kinase pathways in differentiated SH-SY5Y cells. GSK3β protein levels were significantly increased as compared to controls following 24 h exposure of SH-SY5Y cells to PFOS at 0.001 µM concentration, p=0.012 analyzed by the one-way ANOVA (Figure 5A, B). We did not observe any significant changes in CDK5 protein levels and mRNA expression levels of GSK3β and CDK5 (Figure 5C-F), based on a one-way ANOVA followed by Dunnett's for multiple comparisons.

PFOS effects on ApoE and ApoE4 protein levels in differentiated SH-SY5Y cells (Non-neural Pathway)

We further analyzed the impact of PFOS exposure on non-neural pathways associated with AD. SH-SY5Y cells exposed to PFOS at 0.001 µM concentration for 24 h, showed a significant increase in ApoE4 protein levels as compared to controls, P= 0.026 (Figure 6C, D) analyzed by the one-way ANOVA followed by Dunnett's for multiple comparisons. Interestingly, PFOS had no effect on total ApoE protein levels in SH-SY5Y exposed cells at 0.001 and 0.1 µM concentrations following 24 h of exposure (Figure 6A, B).

Effects of developmental exposure of PFOS on APP mRNA expression, APP protein levels, $A\beta_{1-42}$ and $A\beta_{1-40}$ accumulation (amyloidogenic pathway)

We observed an increasing trend in the effect of PFOS exposure on APP mRNA expression and APP protein levels as compared to controls (Figure 7A-C). PFOS exposure caused an increased trend in $A\beta_{42}$ and the ratio of $A\beta_{42}/A\beta_{40}$ proteins levels, however, these findings were not statistically significant. The $A\beta_{40}$ protein levels were not affected (Figure 7D-F).

Effects of developmental PFOS exposure on Tau mRNA expression, Total Tau and P-tau protein levels (tau Pathway)

Tau mRNA expression in the cortex of PFOS exposed group showed no significant difference as compared to controls (Figure 8C). Western blot analysis showed no significant difference between the PFOS exposed group and the control group in Total tau and P-tau (Ser-404) protein levels (Figure 8A, B, D, E). The protein level of P-tau (Thr-181) was trending higher in the PFOS exposed group compared to controls (Figure 8F, G). The PFOS exposed group showed a significant increase in GSK3β protein levels as compared to control group, $p = 0.05$ determined by two-tailed unpaired t-test (Figure 9A, B). The GSK3β mRNA expression was trending higher in the PFOS exposed group compared to controls (Figure 9C). We did not observe any significant effects on CDK5 mRNA expression and protein levels in the PFOS treated group compared with the control group (Figure 9D-F).

Effects of developmental PFOS exposure on ApoE protein levels (Non-neural Pathway)

Western blot analysis showed that PFOS significantly increased total ApoE protein levels in brain cortex as compared to the control group, $p = 0.0025$ analyzed by two-tailed unpaired t-test (Figure 10A, B).

DISCUSSION

As a persistent organic pollutant, PFOS has been identified as a developmental neurotoxicant[24,41,42]. Previous studies have reported the developmental effects of PFOS on neurological disorders, behavioral disorders, and cognitive function[35,43,44]. A few reports indicated that developmental exposure to PFOS induced tau protein levels[37] and enhanced AD pathological hallmarks[45]. However, the effects of PFOS on amyloidogenic, tau, kinase, and non-neural pathways related to AD are not fully elucidated in the literature.

Previous work from our lab has demonstrated that developmental exposure to environmental toxins such as lead (Pb) induced cognitive deficits, latent overexpression of tau, and phosphorylated tau in the adult rodents cortex[46,47]. In addition, differentiated human neuroblastoma cells (SH-SY5Y) exposed to a series of Pb concentrations (0-100 μM) for 48 h showed an alteration in tau and hyperphosphorylation of tau[48]. Therefore, we performed *in vivo* and *in vitro* studies to investigate potential PFOS impacts on AD related biomarkers and pathways.

The present study established that the concentrations range of PFOS (0-100 μM) had no significant cytotoxicity on differentiated SH-SY5Y cells following 24 h of exposure (Figure 2), and revealed that PFOS may impact the amyloidogenic pathway which was indicated by elevation of amyloid precursor protein (APP) levels (Figure 3A, B) at 0.001 μM of PFOS in SH-SY5Y cells. Furthermore, overexpression of tau and site-specific hyperphosphorylation of tau (Ser-404 and Thr181) proteins were both induced by PFOS in SHSY5Y cells at very low concentrations (0.001and 0.1 μM) (Figure 4A, B, D-G) providing more evidence that PFOS can promote AD pathogenesis through modulating the tau pathway. The upregulation of total tau and the abnormal hyperphosphorylation of tau

(P-tau) proteins are responsible for the loss of microtubule stability and axonal transport in AD[49,50]. This is consistent with the study by Zhang et al (2016) which reported that developmental exposure to PFOS induced β-amyloid aggregation, total tau, and phosphorylated tau proteins levels in adult rats at PND 90[45]. Also, Johansson et al (2009) reported that neonatal mice exposed to a single PFOS dose on PND 10 showed a significant elevation of cerebral tau protein levels[37]. This is consistent with our data suggesting the impact of PFOS on amyloidogenic and tau pathways related to AD.

Moreover, we investigated the effect of PFOS on the kinase pathways that are associated with AD. GSK3β is an active serine/threonine proline-directed kinase, it is involved in many processes including inflammatory responses, memory impairment, cholinergic deficits, increased the production of Aβ and hyperphosphorylation of tau[51]. Also, the sites of tau phosphorylation found in AD brain are proline-directed (Thr-Pro or Ser-Pro). Thus, GSK3β plays an important role in the pathogenesis of AD[52]. In this study, we observed the ability of PFOS to promote an increase in the GSK3β protein levels at very low concentrations (0.001 μM; Figure 5A, B). There was no effect observed on CDK5 (Figure 5D-F).

In addition to the most common neural pathways associated with AD, this study to our knowledge is the first study to investigate the effect of PFOS on non-neural pathways associated with AD, namely Apolipoprotein E (ApoE). It has been reported that ApoE4 can stimulate the phosphorylation of tau and the generation of NFTs[18] as well as facilitating the aggregation of Aβ and formation of senile plaque[9,10,11,17]. Also, a recent *in vitro* study indicated that GSK3β activity can be upregulated by ApoE4 through the inhibition of the wnt signaling pathway via Low-density lipoprotein-related protein-5 and -6 (LRP5 and

LRP6) receptors[53]. The *invitro* work here showed that PFOS exposure at 0.001 µM for 24 h increased ApoE4 protein levels significantly (Figure 6C, D). It is worth noting here that our *in vivo* findings did not demonstrate that PFOS exposure alters amyloidogenic and tau pathways in wild-type CD-1 mice on PND 20 (Figure 7 and 8). Similar to previous developmental behavioral study by Butenhoff et al 2009 indicated that rat offspring exposed from GD0 to PND 20 to 1 mg/kg/day PFOS didn't show any changes in learning and memory abilities on PND 20[54]. However, this is in contrast with what was previously published by Zhang et al 2016 and Johansson et al 2009. Thereby, It should be pointed out that in our study PFOS was given to dams via oral gavage and we focused on perinatal exposure of pups to PFOS during gestation and lactation till PND 20, the study by Zhang et al 2016 the dams were given PFOS in drinking water and they studied both perinatal exposure of pups and direct exposure till PND 90. Therefore, the complex physiological activities during the brain developmental stages including the brain growth spurt (BGS) and the establishment of the BBB, as well as the experimental design, time points, animal model, and the duration of exposure might explain the differences in the findings.

Furthermore, our *in vivo* data showed that developmental exposure to PFOS caused a significant increase in GSK3β protein levels (Figure 9A, B). PFOS resulted in a significant elevation of ApoE protein levels in the cerebral cortex of wild-type CD-1 mice (Figure 10A, B). It is noteworthy here that humans express 3 isoforms of ApoE (h-ApoE) protein while mice express only one isoform (m-ApoE)[55]. The homology of the amino acid sequences between the h-ApoE and the m-ApoE is only 70%. Although m-ApoE contains the equivalent Arg112/Arg158 residues present in h-ApoE4, several studies have indicated differences between them including that h-ApoE functions as two distinct protein domains

while m-ApoE functions as a single domain protein[56]. However, it has been demonstrated that the m-ApoE is involved in Aβ amyloid deposition in APP transgenic (Tg) mice that develop Aβ aggregation[57,58].

Although our *in vivo* and *in vitro* findings indicated changes in the protein levels of key biomarkers related to major AD associated pathways, PFOS caused no changes in the mRNA expression of these biomarkers in disagreement with Zhang el at 2016 and others[35,59,60] possibly due to differences in the study design as mentioned above. It is also worth noting that effects of PFOS exposure were mainly in the lower concentrations range and for a short duration (24 hours), consistent with previous studies on other cell types that described the dose-response curve of PFOS as a bell-shaped and non-monotonic[35,61]. Liao et al (2008) reported that 1 μM of PFOS resulted in an increase of glutamate-activated current while 100 μM showed a suppressive effect in cultured primary hippocampal neurons[62]. Additionally, it was indicated that the effects of PFOS exposure on other cell types such as HAPI microglial cells and glioma cells generally reach a peak in short periods and then decline suggesting that the cultured cells may develop tolerability to PFOS by some mechanisms[63,64]. It is worth noting here that this study has limitations. Transgenic mice with human APP, Tau, and expressing human ApoE isoforms would further elucidate the mechanism by which PFOS exposure induces AD pathogenesis. Additionally, studying the effect of PFOS exposure on other CNS cells such as microglia and astrocytes can further recapitulate the impact of PFOS on ApoE and to understand the mechanism of PFOS inducing neurodegeneration.

CONCLUSION

The results presented herein suggest that PFOS impacts amyloidogenic, tau, and kinase pathways related to AD particularly in human cells through the upregulation of ApoE4 protein levels via a mechanism associated with GSK3β. This study may contribute to understanding the mechanism by which PFOS triggers AD pathogenesis. However, further investigation is warranted such as examination of potential involvement of phosphatase enzymes, microRNA, cellular degradation pathways including insulin degrading enzymes in the mechanism of PFOS to further confirm these findings and to provide an insight into the neurodegenerative mechanisms induced by PFOS.

ACKNOWLEDGMENTS

This research was supported by the National Institute of Health STEEP grant (number P42ES027706-03S1) awarded to Dr. Lohmann with an AD supplement that was given to Dr. Slitt and Dr. Zawia. The research was made possible by the use of equipment available through the Rhode Island Institutional Development Award (IDeA) Network of Biomedical Research Excellence from the National Institute of General Medical Sciences (P20GM103430). The authors would also like to extend their thanks to the Animal care staff at URI Comparative Biology Resources Center (CBRC) for their assistance with monitoring the health and the feed of the animal during the study, and Sadegh Modaresi for assistance with mice dosing.

Figure 1. Scheme of PFOS exposure in timed-pregnant CD-1 mice. Pregnant mice were given either 1 mg/kg/day PFOS in water with 0.5% Tween-20 or vehicle (0.5% Tween-20 in water) via oral gavage throughout gestation (GD1-GD18 or 19 [birth]) and lactation (birth to postnatal day [PND] 20). Brain tissues were collected from pups at PND 20 (n=4 per treatment group).

Dam Treatments from GD1-PND20

- Standard chow diet-vehicle (0.5% tween-20 in deionized water).
- Standard chow diet-PFOS (1mg/kg/day in deionized water with 0.5% tween).

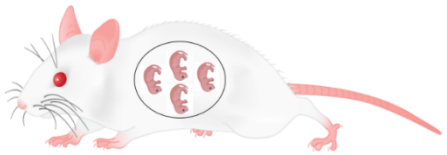

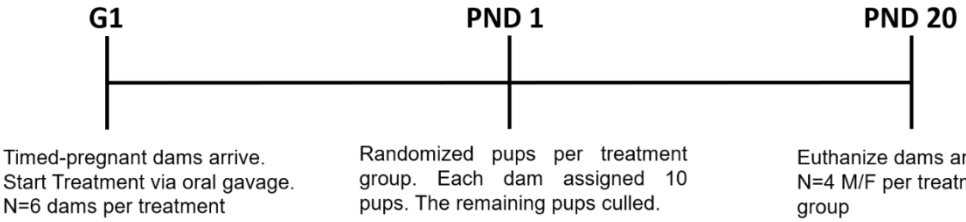

Figure 2. Effects of PFOS exposure on SH-SY5Y cells viability. Cells were exposed to a series of PFOS concentrations (0, 0.001, 0.1, 1, 5, 25, 50, 100 µM) for 24, 48 and 72 h followed by MTS assay. Data are expressed as mean ± S.E.M using the one-way ANOVA followed by Dunnett's for multiple comparisons, n=4 (*P< 0.05, **P< 0.01, ***P< 0.001).

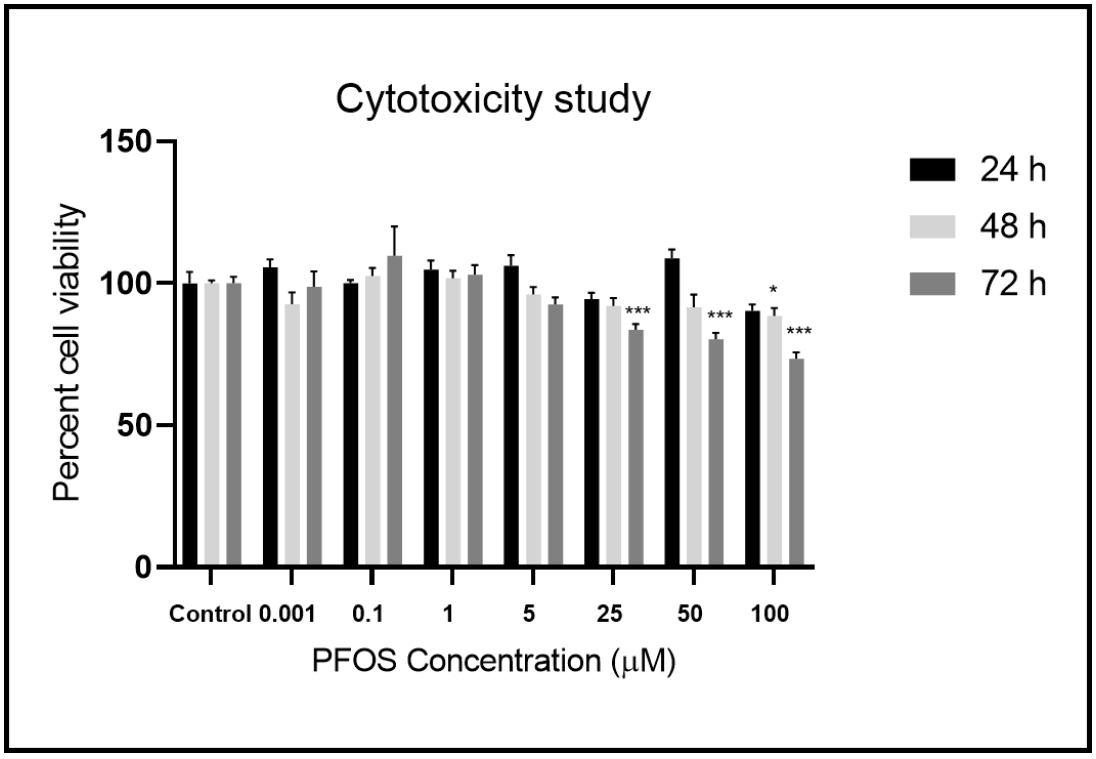
Cytotoxicity study
Percent cell viability
150
100
50
0
24 h
48 h
72 h
***
***
*
***
Control
0.001
0.1
1
5
25
50
100
PFOS Concentration (μM)

Figure 3. APP mRNA and protein levels in differentiated SH-SY5Y cells after PFOS exposure (amyloidogenic pathway). Differentiated SH-SY5Y cells exposed to PFOS at 0.001 and 0.1 µM concentrations for 24 h. (A-B) quantification of APP protein levels normalized to GAPDH. (C) APP mRNA levels. Results are expressed as mean ± S.E.M using the one-way ANOVA followed by Dunnett's for multiple comparisons, n=3 (*P< 0.05, **P< 0.01).

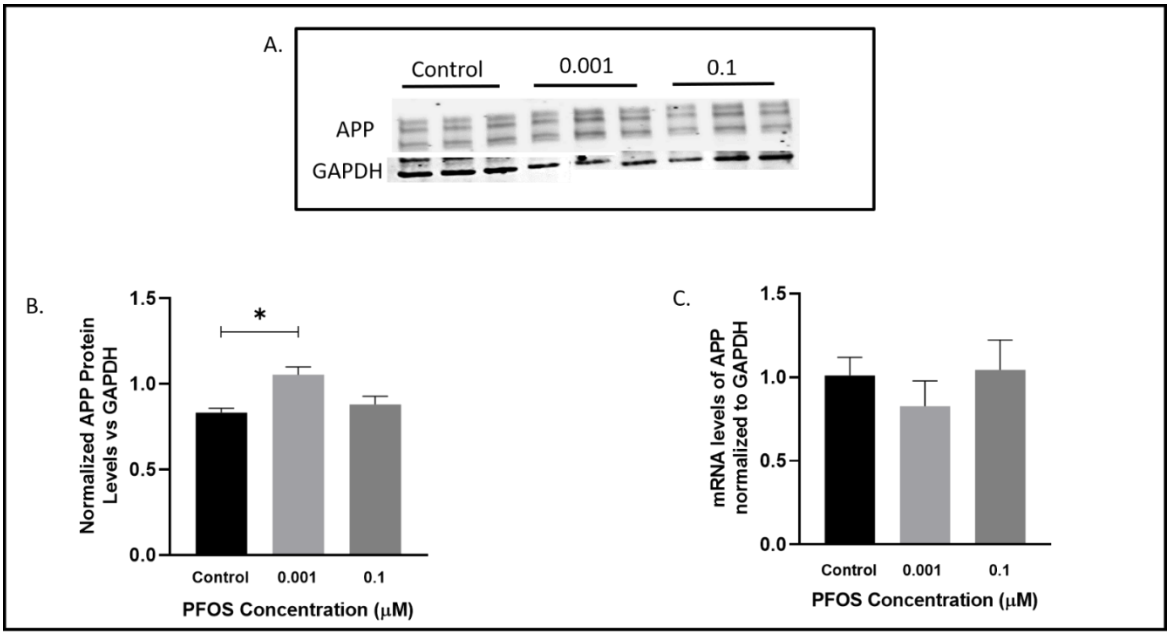
A.
Control
0.001
0.1
APP
GAPDH
B.
Normalized APP Protein Levels vs GAPDH
1.5
1.0
0.5
0.0
*
Control
0.001
0.1
PFOS Concentration (μM)
C.
mRNA levels of APP normalized to GAPDH
1.5
1.0
0.5
0.0
Control
0.001
0.1
PFOS Concentration (μM)

Figure 4. Tau mRNA and protein levels in differentiated SH-SY5Y cells after PFOS exposure (tau pathway). Differentiated SH-SY5Y cells exposed to PFOS at 0.001 and 0.1 µM concentrations for 24 h. (A-B) quantification of Tau protein levels normalized to GAPDH. (C) Tau mRNA levels. (D-E) quantification of p-tau (ser404) protein levels normalized to GAPDH. (F-G) quantification of p-tau (Thr 181) protein levels normalized to GAPDH. Results are expressed as mean ± S.E.M using the one-way ANOVA followed by Dunnett's for multiple comparisons n=3 (*P< 0.05, **P< 0.01).

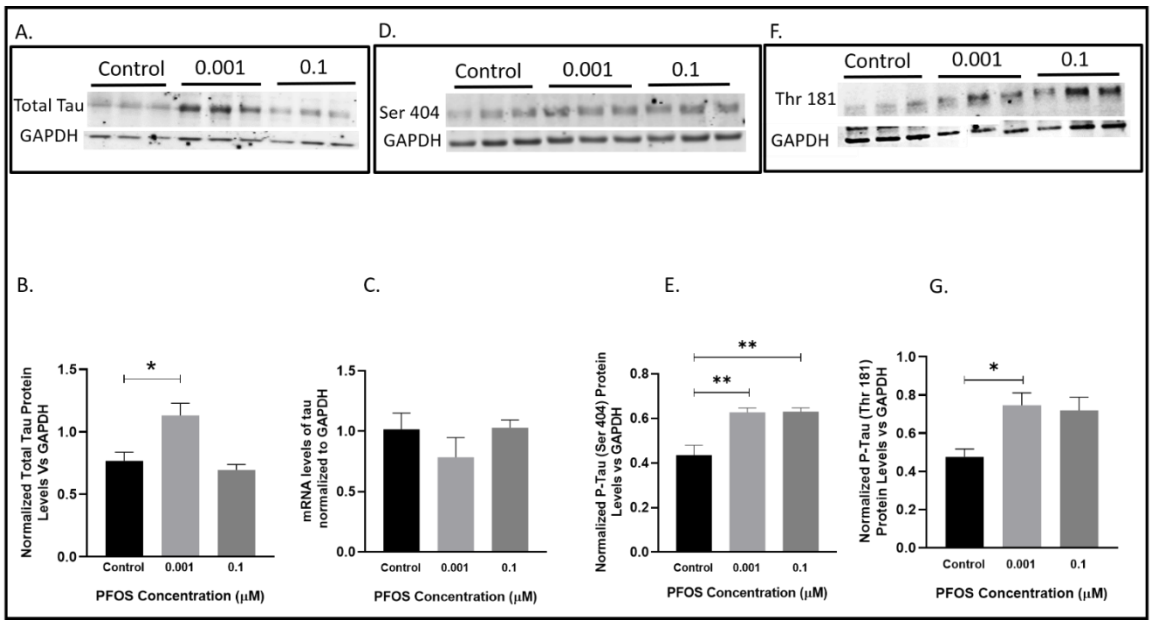
A.
Control
0.001
0.1
Total Tau
GAPDH
D.
Control
0.001
0.1
Ser 404
GAPDH
F.
Control
0.001
0.1
Thr 181
GAPDH
B.
Normalized Total Tau Protein Levels Vs GAPDH
PFOS Concentration (μM)
C.
mRNA levels of tau normalized to GAPDH
PFOS Concentration (μM)
E.
Normalized P-Tau (Ser 404) Protein Levels vs GAPDH
PFOS Concentration (μM)
G.
Normalized P-Tau (Thr 181) Protein Levels vs GAPDH
PFOS Concentration (μM)

Figure 5. **GSK3β, CDK5 mRNA, and protein levels in differentiated SH-SY5Y cells after PFOS exposure (kinase pathway).** Differentiated SH-SY5Y cells exposed to PFOS at 0.001 and 0.1 μM concentrations for 24 h. (A-B) quantification of GSK3β protein levels normalized to GAPDH. (C) GSK3β mRNA levels. (D-E) quantification of CDK5 protein levels normalized to GAPDH. (F) CDK5 mRNA levels. Results are expressed as mean ± S.E.M using the one-way ANOVA followed by Dunnett's for multiple comparisons, n=3 (*P< 0.05, **P< 0.01).

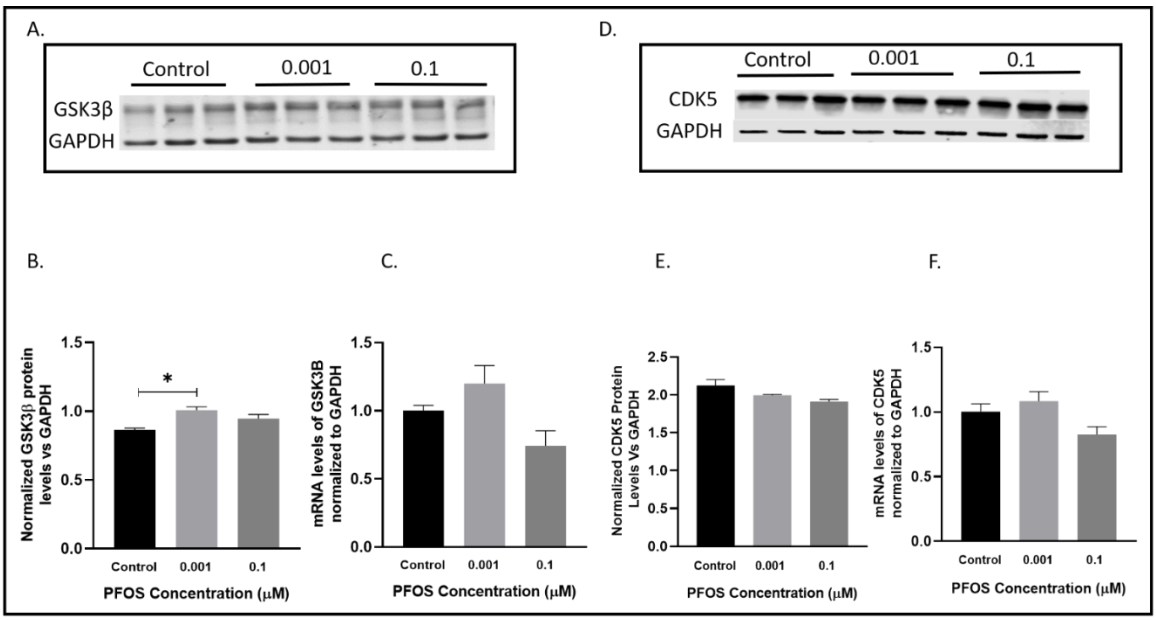
A.
Control
0.001
0.1
GSK3β
GAPDH
D.
Control
0.001
0.1
CDK5
GAPDH
B.
C.
E.
F.
Normalized GSK3β protein levels vs GAPDH
mRNA levels of GSK3B normalized to GAPDH
Normalized CDK5 Protein Levels Vs GAPDH
mRNA levels of CDK5 normalized to GAPDH
PFOS Concentration (μM)
Control
0.001
0.1
*

Figure 6. ApoE protein levels in differentiated SH-SY5Y cells after PFOS exposure (non-neural pathway). Differentiated SH-SY5Y cells exposed to PFOS at 0.001 and 0.1 µM concentrations for 24 h. (A-B) quantification of ApoE protein levels normalized to GAPDH. (C-D) quantification of ApoE4 protein levels normalized to GAPDH. Results are expressed as mean ± S.E.M using the one-way ANOVA followed by Dunnett's for multiple comparisons, n=3 (*P< 0.05, **P< 0.01).

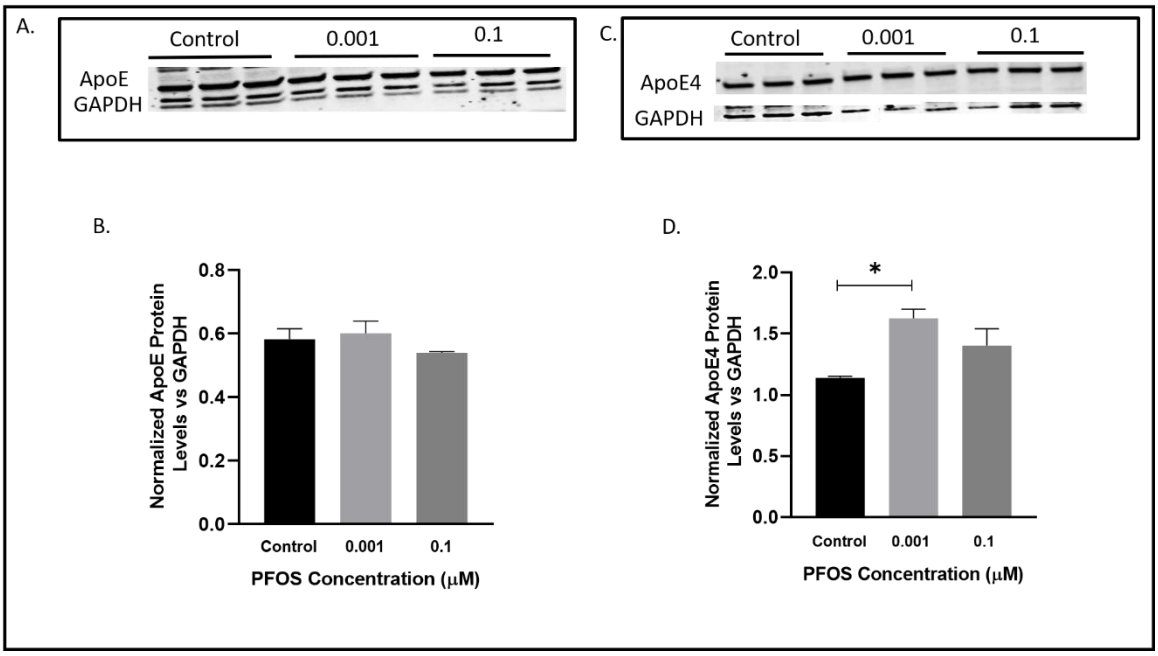
A.
Control
0.001
0.1
ApoE
GAPDH
C.
Control
0.001
0.1
ApoE4
GAPDH
B.
Normalized ApoE Protein Levels vs GAPDH
0.8
0.6
0.4
0.2
0.0
Control
0.001
0.1
PFOS Concentration (μM)
D.
Normalized ApoE4 Protein Levels vs GAPDH
*
2.0
1.5
1.0
0.5
0.0
Control
0.001
0.1
PFOS Concentration (μM)

Figure 7. APP mRNA and protein levels at PND 20 in the cortex of CD-1 pup mice developmentally exposed to PFOS (amyloidogenic pathway). Timed-pregnant female CD-1 mice were administered with vehicle (0.5% Tween-20 in water) or 1 mg/kg/day PFOS in water with 0.5% Tween-20 via oral gavage from gestation GD1 through postnatal day PND 20. (A-B) quantification of APP protein levels normalized to GAPDH. (C) APP mRNA levels. (D-E) quantification of Aβ 1-42 and Aβ 1-40 protein levels normalized to GAPDH. (F) Aβ 1-42: Aβ 1-40 ratio. Results are expressed as mean ± S.E.M using the two-tailed unpaired t-test, n=4. Results were non-significant.

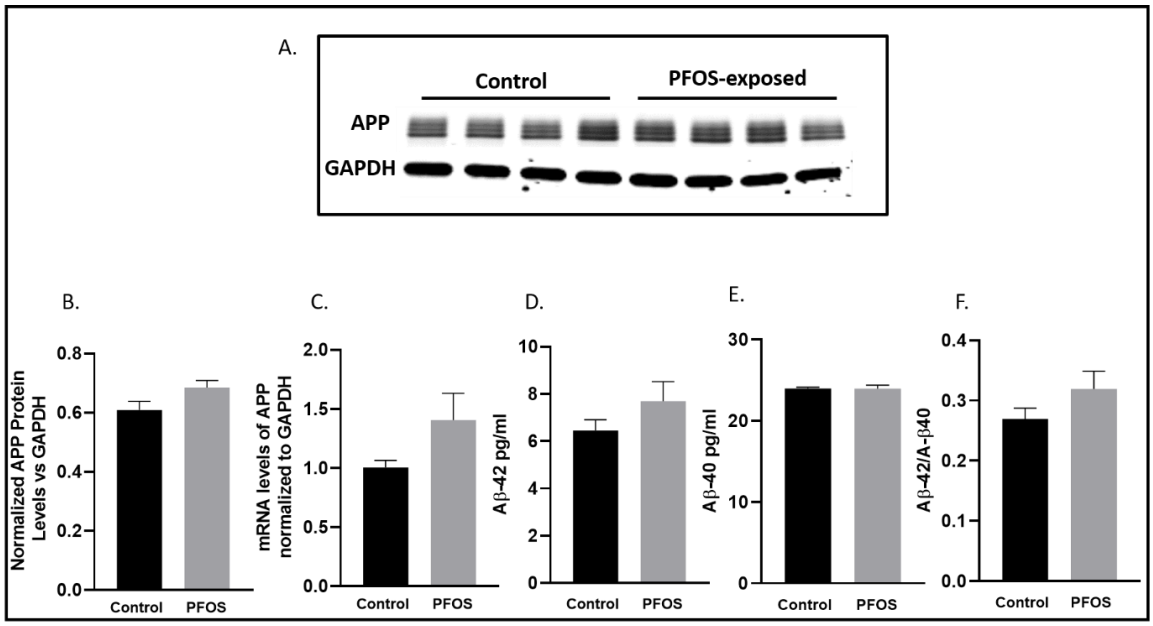
A.
Control
PFOS-exposed
APP
GAPDH
B.
Normalized APP Protein Levels vs GAPDH
0.0
0.2
0.4
0.6
0.8
Control
PFOS
C.
mRNA levels of APP normalized to GAPDH
0.0
0.5
1.0
1.5
2.0
Control
PFOS
D.
Aβ-42 pg/ml
0
2
4
6
8
10
Control
PFOS
E.
Aβ-40 pg/ml
0
10
20
30
Control
PFOS
F.
Aβ-42/A-β40
0.0
0.1
0.2
0.3
0.4
Control
PFOS

Figure 8. Tau mRNA and protein levels at PND 20 in the cortex of CD-1 pup mice developmentally exposed to PFOS (tau pathway). Timed-pregnant female CD-1 mice were administered with vehicle (0.5% Tween-20 in water) or 1 mg/kg/day PFOS in water with 0.5% Tween-20 via oral gavage from gestation GD1 through postnatal day PND 20. (A-B) quantification of Tau protein levels normalized to GAPDH. (C) Tau mRNA levels. (D-E) quantification of p-tau (ser404) protein levels normalized to GAPDH. (F-G) quantification of p-tau (Thr 181) protein levels normalized to GAPDH. Results are expressed as mean ± S.E.M using the two-tailed unpaired t-test, n=4. Results don't indicate a significant difference between the two groups.

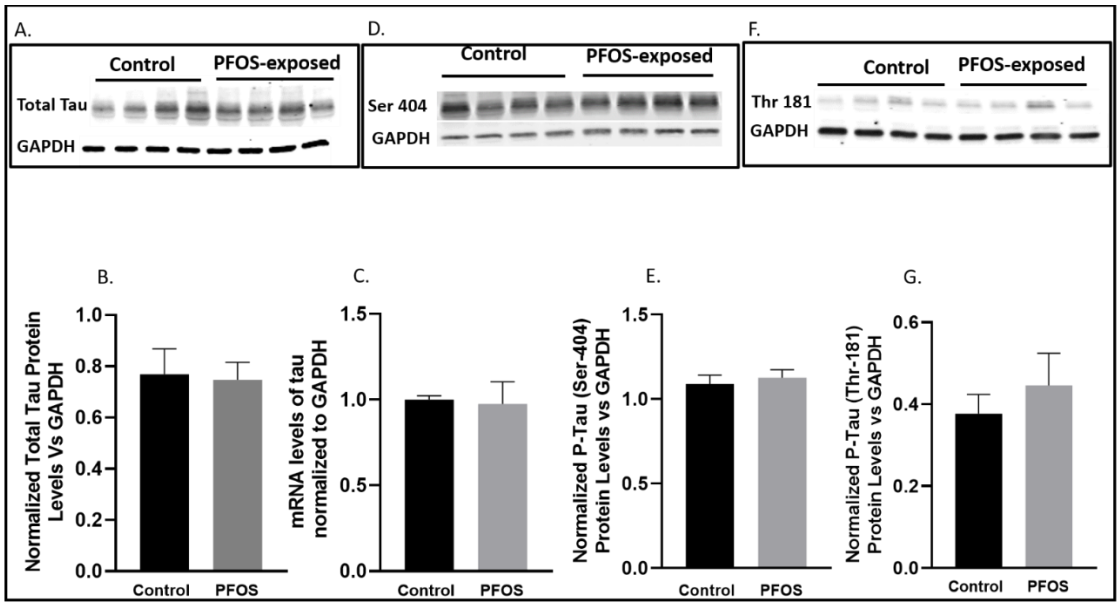
A.
Control
PFOS-exposed
Total Tau
GAPDH
D.
Control
PFOS-exposed
Ser 404
GAPDH
F.
Control
PFOS-exposed
Thr 181
GAPDH
B.
Normalized Total Tau Protein Levels Vs GAPDH
1.0
0.8
0.6
0.4
0.2
0.0
Control
PFOS
C.
mRNA levels of tau normalized to GAPDH
1.5
1.0
0.5
0.0
Control
PFOS
E.
Normalized P-Tau (Ser-404) Protein Levels vs GAPDH
1.5
1.0
0.5
0.0
Control
PFOS
G.
Normalized P-Tau (Thr-181) Protein Levels vs GAPDH
0.6
0.4
0.2
0.0
Control
PFOS

Figure 9. GSK3β, CDK5 mRNA levels and protein levels at PND 20 in the cortex of CD-1 pup mice developmentally exposed to PFOS (kinase pathway). Timed-pregnant female CD-1 mice were administered with vehicle (0.5% Tween-20 in water) or 1 mg/kg/day PFOS in water with 0.5% Tween-20 via oral gavage from gestation GD1 through postnatal day PND 20. (A-B) quantification of GSK3β protein levels normalized to GAPDH. (C) GSK3β mRNA levels. (D-E) quantification of CDK5 protein levels normalized to GAPDH. (F) CDK5 mRNA levels. Results are expressed as mean ± S.E.M using the two-tailed unpaired t-test, n=4 (*P< 0.05, **P< 0.01).

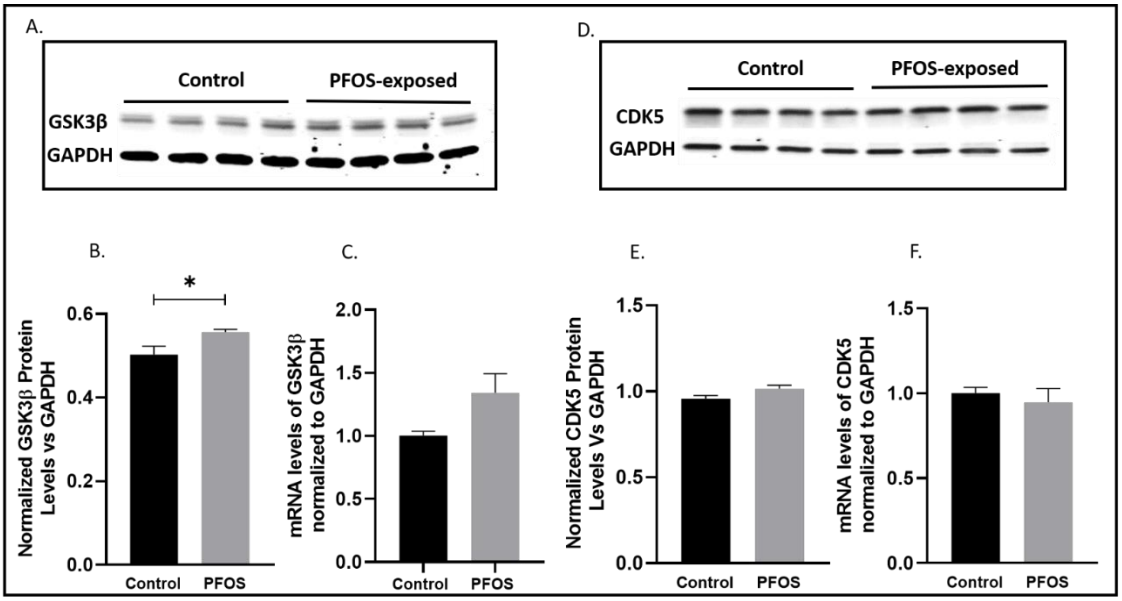
A.
Control
PFOS-exposed
GSK3β
GAPDH
D.
Control
PFOS-exposed
CDK5
GAPDH
B.
*
Normalized GSK3β Protein Levels vs GAPDH
0.6
0.4
0.2
0.0
Control
PFOS
C.
mRNA levels of GSK3β normalized to GAPDH
2.0
1.5
1.0
0.5
0.0
Control
PFOS
E.
Normalized CDK5 Protein Levels Vs GAPDH
1.5
1.0
0.5
0.0
Control
PFOS
F.
mRNA levels of CDK5 normalized to GAPDH
1.5
1.0
0.5
0.0
Control
PFOS

Figure 10. ApoE protein levels at PND 20 in the cortex of CD-1 pup mice developmentally exposed to PFOS (non-neural pathway). Timed-pregnant female CD-1 mice were administered with vehicle (0.5% Tween-20 in water) or 1 mg/kg/day PFOS in water with 0.5% Tween-20 via oral gavage from gestation GD1 through postnatal day PND 20. (A-B) quantification of ApoE protein levels normalized to GAPDH. Results are expressed as mean ± S.E.M using the two-tailed unpaired t-test, n=4 (*P< 0.05, **P< 0.01).

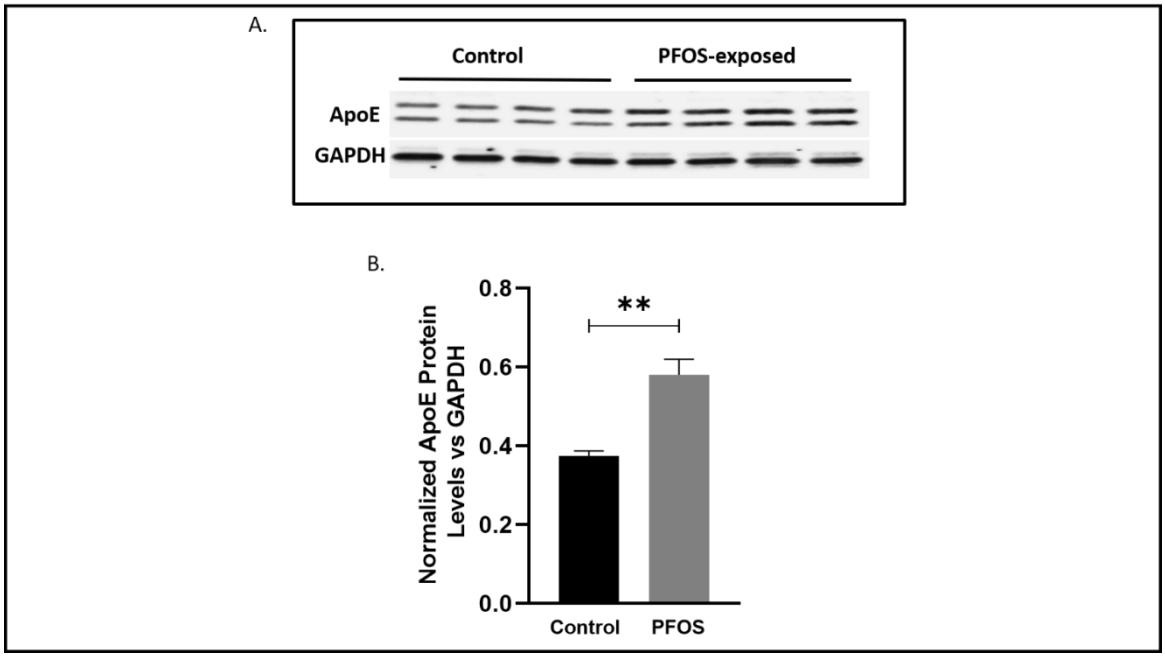
A.
Control
PFOS-exposed
ApoE
GAPDH
B.
Normalized ApoE Protein Levels vs GAPDH
0.8
0.6
0.4
0.2
0.0
**
Control
PFOS

BIBLIOGRAPHY

1. Deture MA, Dickson DW. The neuropathological diagnosis of Alzheimer's disease. *Mol Neurodegener*. 2019;14(1):1-18. doi:10.1186/s13024-019-0333-5
2. American Psychiatric Association (APA). *Diagnostic and Statistical Manual of Mental Disorders*. 5th ed. Arlington, VA; 2013. doi:10.1176/appi.books.9780890425596
3. Manoharan S, Guillemin GJ, Abiramasundari RS, Essa MM, Akbar M, Akbar MD. The Role of Reactive Oxygen Species in the Pathogenesis of Alzheimer's Disease, Parkinson's Disease, and Huntington's Disease: A Mini Review. *Oxid Med Cell Longev*. 2016;2016. doi:10.1155/2016/8590578
4. Murphy MP, Levine H. Alzheimer's Disease and the Beta-Amyloid Peptide. *J Alzheimer's Dis*. 2010;19(1):1-17. doi:10.3233/JAD-2010-1221.Alzheimer
5. Garcia ML, Cleveland DW. Going new places using an old MAP : tau , microtubules and human neurodegenerative disease. :41-48.
6. Drahansky M, Paridah M., Moradbak A, et al. We are IntechOpen , the world ' s leading publisher of Open Access books Built by scientists , for scientists TOP 1 %. *Intech*. 2016;i(tourism):13. doi:http://dx.doi.org/10.5772/57353
7. Haider W, Lackner F, Tonczar L. Verabreichung Hochprozentiger Glucose Mit Grossen Insulindosen Im Rahmen Einer Fruhzeitigen Totalen Parenteral Ernahrung Bei Patienten Mit Schockbedingtem Ubersteigerten Kalorienbedarf. *Anaesthesist*. 1975;24(7):289-298.
8. Martin L, Latypova X, Wilson CM, et al. Tau protein kinases: Involvement in Alzheimer's disease. *Ageing Res Rev*. 2013;12(1):289-309.

doi:10.1016/j.arr.2012.06.003

9. Verghese PB, Castellano JM, Holtzman DM. Apolipoprotein E in Alzheimer's disease and other neurological disorders. *Lancet Neurol*. 2011;10(3):241-252. doi:10.1016/S1474-4422(10)70325-2

10. Fan X, Gaur U, Yang M. Aging and Aging-Related Diseases. *Adv Exp Med Biol*. 2018;1086:157-168. doi:10.1007/978-981-13-1117-8

11. Koffie RM, Hashimoto T, Tai HC, et al. Apolipoprotein E4 effects in Alzheimer's disease are mediated by synaptotoxic oligomeric amyloid-β. *Brain*. 2012;135(7):2155-2168. doi:10.1093/brain/aws127

12. Pfrieger FW. Cholesterol homeostasis and function in neurons of the central nervous system. *Cell Mol Life Sci*. 2003;60(6):1158-1171. doi:10.1007/s00018-003-3018-7

13. Huang YWA, Zhou B, Wernig M, Südhof TC. ApoE2, ApoE3, and ApoE4 Differentially Stimulate APP Transcription and Aβ Secretion. *Cell*. 2017;168(3):427-441.e21. doi:10.1016/j.cell.2016.12.044

14. Zannis VI, Breslow JL, Utermann G, et al. Note Nmenclature. *J Lipid Res*. 1982;23:911-914.

15. Huang Y, Liu XQ, Wyss-Coray T, Brecht WJ, Sanan DA, Mahley RW. Apolipoprotein E fragments present in Alzheimer's disease brains induce neurofibrillary tangle-like intracellular inclusions in neurons. *Proc Natl Acad Sci U S A*. 2001;98(15):8838-8843. doi:10.1073/pnas.151254698

16. Brecht WJ, Harris FM, Chang S, et al. Neuron-Specific Apolipoprotein E4 Proteolysis Is Associated with Increased Tau Phosphorylation in Brains of

Transgenic Mice. *J Neurosci*. 2004;24(10):2527-2534. doi:10.1523/JNEUROSCI.4315-03.2004

17. Office H, Factory M, Office S, Office B, Office D. LAN Cable. 2010;10(5):333-344. doi:10.1038/nrn2620.Apolipoprotein

18. Huang Y. Aβ-independent roles of apolipoprotein E4 in the pathogenesis of Alzheimer's disease. *Trends Mol Med*. 2010;16(6):287-294. doi:10.1016/j.molmed.2010.04.004

19. Tai LM, Bilousova T, Jungbauer L, et al. Levels of soluble apolipoprotein E/amyloid-β (Aβ) complex are reduced and oligomeric Aβ increased with APOE4 and alzheimer disease in a transgenic mouse model and human samples. *J Biol Chem*. 2013;288(8):5914-5926. doi:10.1074/jbc.M112.442103

20. Hashimoto T, Serrano-Pozo A, Hori Y, et al. Apolipoprotein e, especially apolipoprotein E4, increases the oligomerization of amyloid β peptide. *J Neurosci*. 2012;32(43):15181-15192. doi:10.1523/JNEUROSCI.1542-12.2012

21. Höglund K, Kern S, Zettergren A, et al. Preclinical amyloid pathology biomarker positivity: Effects on tau pathology and neurodegeneration. *Transl Psychiatry*. 2017;7(1):1-7. doi:10.1038/tp.2016.252

22. Dash M, Eid A, Subaiea G, et al. Developmental exposure to lead (Pb) alters the expression of the human tau gene and its products in a transgenic animal model. *Neurotoxicology*. 2016;55:154-159. doi:10.1016/j.neuro.2016.06.001

23. Wang Y, Wang L, Chang W, Zhang Y, Zhang Y, Liu W. Neurotoxic effects of perfluoroalkyl acids: Neurobehavioral deficit and its molecular mechanism. *Toxicol Lett*. 2019;305(January):65-72. doi:10.1016/j.toxlet.2019.01.012

24. Lau C, Anitole K, Hodes C, Lai D, Pfahles-Hutchens A, Seed J. Perfluoroalkyl acids: A review of monitoring and toxicological findings. *Toxicol Sci*. 2007;99(2):366-394. doi:10.1093/toxsci/kfm128

25. Mondal D, Lopez-Espinosa MJ, Armstrong B, Stein CR, Fletcher T. Relationships of perfluorooctanoate and perfluorooctane sulfonate serum concentrations between mother-child pairs in a population with perfluorooctanoate exposure from drinking water. *Environ Health Perspect*. 2012;120(5):752-757. doi:10.1289/ehp.1104538

26. Lau C, Butenhoff JL, Rogers JM. The developmental toxicity of perfluoroalkyl acids and their derivatives. *Toxicol Appl Pharmacol*. 2004;198(2):231-241. doi:10.1016/j.taap.2003.11.031

27. Lau C, Thibodeaux JR, Hanson RG, et al. Effects of perfluorooctanoic acid exposure during pregnancy in the mouse. *Toxicol Sci*. 2006;90(2):510-518. doi:10.1093/toxsci/kfj105

28. Lau C, Anitole K, Hodes C, Lai D, Pfahles-Hutchens A, Seed J. Perfluoroalkyl acids: A review of monitoring and toxicological findings. *Toxicol Sci*. 2007;99(2):366-394. doi:10.1093/toxsci/kfm128

29. Winkens K, Vestergren R, Berger U, Cousins IT. Early life exposure to per- and poly fl uoroalkyl substances (PFASs): A critical review. *Emerg Contam*. 2017;3(2):55-68. doi:10.1016/j.emcon.2017.05.001

30. Forsthuber M, Kaiser AM, Granitzer S, et al. Albumin is the major carrier protein for PFOS, PFOA, PFHxS, PFNA and PFDA in human plasma. *Environ Int*. 2020;137(February):105324. doi:10.1016/j.envint.2019.105324

31. Olsen GW, Burris JM, Ehresman DJ, et al. Half-Life of Serum Elimination of

Perfluorooctanesulfonate , Perfluorohexanesulfonate , and Perfluorooctanoate in Retired Fluorochemical Production Workers. 2007;(9):1298-1305. doi:10.1289/ehp.10009

32. Chang SC, Noker PE, Gorman GS, et al. Comparative pharmacokinetics of perfluorooctanesulfonate (PFOS) in rats, mice, and monkeys. *Reprod Toxicol*. 2012;33(4):428-440. doi:10.1016/j.reprotox.2011.07.002

33. Zeng H cai, Zhang L, Li Y yuan, et al. Inflammation-like glial response in rat brain induced by prenatal PFOS exposure. *Neurotoxicology*. 2011;32(1):130-139. doi:10.1016/j.neuro.2010.10.001

34. Johansson N, Fredriksson A, Eriksson P. Neonatal exposure to perfluorooctane sulfonate (PFOS) and perfluorooctanoic acid (PFOA) causes neurobehavioural defects in adult mice. *Neurotoxicology*. 2008;29(1):160-169. doi:10.1016/j.neuro.2007.10.008

35. Wang Y, Liu W, Zhang Q, Zhao H, Quan X. Effects of developmental perfluorooctane sulfonate exposure on spatial learning and memory ability of rats and mechanism associated with synaptic plasticity. *Food Chem Toxicol*. 2015;76:70-76. doi:10.1016/j.fct.2014.12.008

36. Fuentes S, Colomina MT, Vicens P, Franco-Pons N, Domingo JL. Concurrent exposure to perfluorooctane sulfonate and restraint stress during pregnancy in mice: Effects on postnatal development and behavior of the offspring. *Toxicol Sci*. 2007;98(2):589-598. doi:10.1093/toxsci/kfm121

37. Johansson N, Eriksson P, Viberg H. Neonatal exposure to PFOS and PFOA in mice results in changes in proteins which are important for neuronal growth and

synaptogenesis in the developing brain. *Toxicol Sci*. 2009;108(2):412-418. doi:10.1093/toxsci/kfp029

38. Fuentes S, Vicens P, Colomina MT, Domingo JL. Behavioral effects in adult mice exposed to perfluorooctane sulfonate (PFOS). *Toxicology*. 2007;242(1-3):123-129. doi:10.1016/j.tox.2007.09.012

39. Zhang Q, Zhao H, Liu W, et al. Developmental perfluorooctane sulfonate exposure results in tau hyperphosphorylation and β-amyloid aggregation in adults rats: Incidence for link to Alzheimer's disease. *Toxicology*. 2016;347-349:40-46. doi:10.1016/j.tox.2016.03.003

40. Bihaqi SW, Alansi B, Masoud AM, Mushtaq F, Subaiea GM, Zawia NH. Influence of Early Life Lead (Pb) Exposure on α-Synuclein, GSK-3β and Caspase-3 Mediated Tauopathy: Implications on Alzheimer's Disease. *Curr Alzheimer Res*. 2018;15(12):1114-1122. doi:10.2174/1567205015666180801095925

41. Lau C, Thibodeaux JR, Hanson RG, et al. Exposure to perfluorooctane sulfonate during pregnancy in rat and mouse. II: Postnatal evaluation. *Toxicol Sci*. 2003;74(2):382-392. doi:10.1093/toxsci/kfg122

42. Luebker DJ, Case MT, York RG, Moore JA, Hansen KJ, Butenhoff JL. Two-generation reproduction and cross-foster studies of perfluorooctanesulfonate (PFOS) in rats. *Toxicology*. 2005;215(1-2):126-148. doi:10.1016/j.tox.2005.07.018

43. Long Y, Wang Y, Ji G, Yan L, Hu F, Gu A. Neurotoxicity of Perfluorooctane Sulfonate to Hippocampal Cells in Adult Mice. *PLoS One*. 2013;8(1):1-9. doi:10.1371/journal.pone.0054176

44. Sun P, Gu L, Luo J, Qin Y, Sun L, Jiang S. ROS-mediated JNK pathway critically

contributes to PFOS-triggered apoptosis in SH-SY5Y cells. *Neurotoxicol Teratol*. 2019;75(July):106821. doi:10.1016/j.ntt.2019.106821

45. Zhang Q, Zhao H, Liu W, et al. Developmental per fl uorooctane sulfonate exposure results in tau hyperphosphorylation and b -amyloid aggregation in adults rats : Incidence for link to Alzheimer ' s disease. *Toxicology*. 2016;347-349:40-46. doi:10.1016/j.tox.2016.03.003

46. Bihaqi SW, Bahmani A, Subaiea GM, Zawia NH. Infantile exposure to lead and late-age cognitive decline: Relevance to AD. *Alzheimer's Dement*. 2014;10(2):187-195. doi:10.1016/j.jalz.2013.02.012

47. Bihaqi SW, Bahmani A, Adem A, Zawia NH. Infantile postnatal exposure to lead (Pb) enhances tau expression in the cerebral cortex of aged mice: Relevance to AD. *Neurotoxicology*. 2014;44:114-120. doi:10.1016/j.neuro.2014.06.008

48. Bihaqi SW, Eid A, Zawia NH. Lead exposure and tau hyperphosphorylation: An in-Vitro study. *Neurotoxicology*. 2017;62:218-223. doi:10.1016/j.neuro.2017.07.029

49. Salehi A, Delcroix JD, Mobley WC. Traffic at the intersection of neurotrophic factor signaling and neurodegeneration. *Trends Neurosci*. 2003;26(2):73-80. doi:10.1016/S0166-2236(02)00038-3

50. Dubey J, Ratnakaran N, Koushika SP. Neurodegeneration and microtubule dynamics: Death by a thousand cuts. *Front Cell Neurosci*. 2015;9(September):1-15. doi:10.3389/fncel.2015.00343

51. Hoshi M, Takashima A, Noguchi K, et al. Regulation of mitochondrial pyruvate dehydrogenase activity by tau protein kinase I/glycogen synthase kinase 3β in

brain. *Proc Natl Acad Sci U S A*. 1996;93(7):2719-2723. doi:10.1073/pnas.93.7.2719

52. Hooper C, Killick R, Lovestone S. The GSK3 hypothesis of Alzheimer's disease. *J Neurochem*. 2008;104(6):1433-1439. doi:10.1111/j.1471-4159.2007.05194.x

53. Caruso A, Motolese M, Iacovelli L, et al. Inhibition of the canonical Wnt signaling pathway by apolipoprotein E4 in PC12 cells. 2006:364-371. doi:10.1111/j.1471-4159.2006.03867.x

54. Butenhoff JL, Ehresman DJ, Chang SC, Parker GA, Stump DG. Gestational and lactational exposure to potassium perfluorooctanesulfonate (K+PFOS) in rats: Developmental neurotoxicity. *Reprod Toxicol*. 2009;27(3-4):319-330. doi:10.1016/j.reprotox.2008.12.010

55. Lewandowski CT, Maldonado Weng J, LaDu MJ. Alzheimer's disease pathology in APOE transgenic mouse models: The Who, What, When, Where, Why, and How. *Neurobiol Dis*. 2020;139(February):104811. doi:10.1016/j.nbd.2020.104811

56. Nguyen D, Dhanasekaran P, Nickel M, et al. Influence of domain stability on the properties of human apolipoprotein E3 and E4 and mouse apolipoprotein e. *Biochemistry*. 2014;53(24):4025-4033. doi:10.1021/bi500340z

57. Fagan AM, Watson M, Parsadanian M, Bales KR, Paul SM, Holtzman DM. Human and Murine ApoE Markedly Alters A □ Metabolism before and after Plaque Formation in a Mouse Model of Alzheimer ' s Disease. 2002;318:305-318. doi:10.1006/nbdi.2002.0483

58. Bales KR, Verina T, Cummins DJ, et al. Apolipoprotein E is essential for amyloid deposition in the APP(V717F) transgenic mouse model of Alzheimer's disease.

Proc Natl Acad Sci U S A. 1999;96(26):15233-15238. doi:10.1073/pnas.96.26.15233

59. Li W, He QZ, Wu CQ, et al. PFOS Disturbs BDNF-ERK-CREB Signalling in Association with Increased MicroRNA-22 in SH-SY5Y Cells. *Biomed Res Int*. 2015;2015. doi:10.1155/2015/302653

60. Guo XX, He QZ, Li W, et al. Brain-derived neurotrophic factor mediated perfluorooctane sulfonate induced-neurotoxicity via epigenetics regulation in SK-N-SH cells. *Int J Mol Sci*. 2017;18(4):1-13. doi:10.3390/ijms18040893

61. Chen X, Nie X, Mao J, Zhang Y, Yin K, Jiang S. Perfluorooctanesulfonate induces neuroinflammation through the secretion of TNF-α mediated by the JAK2/STAT3 pathway. *Neurotoxicology*. 2018;66:32-42. doi:10.1016/j.neuro.2018.03.003

62. Liao C yang, Cui L, Zhou Q fang, Duan S min, Jiang G bin. Effects of perfluorooctane sulfonate on ion channels and glutamate-activated current in cultured rat hippocampal neurons. *Environ Toxicol Pharmacol*. 2009;27(3):338-344. doi:10.1016/j.etap.2008.11.013

63. Chen X, Nie X, Mao J, Zhang Y, Yin K, Jiang S. Per fl uorooctanesulfonate induces neuroin fl ammation through the secretion of TNF- a mediated by the JAK2 / STAT3 pathway. 2018;66:32-42.

64. Yang J, Wang C, Nie X, et al. Perfluorooctane sulfonate mediates microglial activation and secretion of TNF-α through Ca2 +-dependent PKC-NF-kB signaling. *Int Immunopharmacol*. 2015;28(1):52-60. doi:10.1016/j.intimp.2015.05.019